Analysing and comparing the intra-halo region in Milky Way-like simulations

Isak Lindh

Division of Astrophysics
Department of Physics

LUND UNIVERSITY

2024–EXA222

Degree project of 15 higher education credits
May 2024

Supervisors: Santi Roca Fàbrega, Tilly Evans-Hofmann & Oscar Agertz

Division of Astrophysics
Department of Physics
Box 118
SE-221 00 Lund
Sweden

Abstract

Dark matter has an important role in our Universe, especially in galaxy formation and evolution, but there are many theoretical models that attempt to describe it and to find out which one, if any, are correct we must test them. Testing a theoretical model of this nature at a galactic scale must and has been done using computational methods through simulations, but this has revealed more complicated problems. One of the more successful of the models is the cold dark matter (CDM) model, assuming non-relativistic dark matter velocities, but it still has problems, such as at smaller scales.

Testing models can be done in several different ways, such as changing the dark matter species i.e. particle type, but in this work the focus was on the effects of using slightly different baryonic physics on the distribution of matter, mostly stars, outside the disc and bulge in the so called intra-halo region (IHR). The light from the stars in this IHR, referred to as the intra-halo light (IHL) in this work, is expected to be correlated to the assembly history of the galaxy which in turn depends strongly on the properties of dark matter.

To test the baryonic physics in the IHR, an analysis and comparison of different galaxy simulations produced by the different codes ART-I, CHANGA, ENZO, GADGET-3, GEAR, GIZMO, and finally AREPO was done. All of these simulations were at a redshift of $z = 4$, had the same initial conditions, very similar physics, and Milky Way-like mass. They were all produced and provided by the AGORA Collaboration assuming a Λ-CDM cosmological model with a matter density of $\Omega_m = 0.272$, a vacuum density of $\Omega_\Lambda = 0.728$, and a Hubble constant of $H_0 = 70.2$ km s^{-1}.

The first goal of this thesis was to produce radial profiles of the gas, stars, and dark matter belonging to the simulations from each code and compare these to similar ones produced by AGORA in order to both confirm their reproducibility and ensure that they were correct. The absolute majority of them had a strong resemblance, and many results were reproduced, but some discrepancies were found. While the exact source of the differences could not be properly discerned, they were most likely due to complications with the analysis tool `yt`.

The second goal was to isolate the IHR and again produce and compare radial profiles of the gas, stars, and dark matter but now only this region. This showed that the method of isolating the IHR using a transition radius based on the virial radius of the galaxy/satellite was effective in removing large quantities of matter but had, as expected, some problems with accuracy. Comparing the radial profiles revealed that most of them had a very strong similarity to the counterpart in the whole galaxy but with more noise. The source of the noise was most likely due to the decrease in sample size but could, for some of the properties, also be a characteristic of the IHR.

This work was partly intended as a preparatory work to in future assist in separating the effects of different baryonic physics from the change in dark matter properties which could hopefully reveal more about dark matter itself.

Populärvetenskaplig Beskrivning

Universum är en underlig plats som har ställt många frågor, vissa som vi svarat på men många är kvar och ännu fler är okända. En av de som vi aktivt börjat besvara är frågan om mörk materia. Hur vet vi att det finns? Hur kan vi veta mer? Vad är det? Den första av dessa delfrågor har vi redan besvarat, vi vet att mörk materia finns för att det behövs någon osynlig massa för att, bland annat, rotationshastigheterna av materia runtom galaxer, så som vår egen Vintergatan, ska vara rimliga och de massiva strukturer som vi observerar, så som galaxer och galaxhopar, ska kunna vara stabila. Men för att förstå dessa fenomen så måste vi veta mer om mörk materia, och genom att den verkar ha en stor roll för galaxer så ligger kanske svaret i deras formation och utveckling.

Men frågan är då, hur kan vi veta mer? En av problemen med att lära oss mer om mörk materia är att vi har skapat många olika teoretiska modeller men vi kan inte dem experimentellt, så som många andra grenar av fysik kan, utan vi förlitar oss på observationer och beräkningsmetoder. Observationer är däremot för det mesta uteslutet då de är väldigt begränsade, både med vår teknologi men också för att vi ser endast galaxer i en av dess många faser. Därför har vi vänt oss mot beräkningsmetoder, mer specifikt simulationer.

Detta arbete fokuserade på att använda dessa simulationer av galaxer, mer specifikt Vintergatan-liknande galaxer, och deras utveckling i syfte att undersöka egenskaperna hos dess gas, stjärnor och mörka materia i dess bula, disk, och halo. Detta gjordes först för att jämföra med resultaten från gruppen forskare som gav datan vid namn the AGORA (Assembling Galaxies Of Resolved Astronomy) Collaboration. De fokuserar på att verifiera att de beräkningsmetoder som används för simulationskoderna producerar samma resultat oberoende på tillvägagångsätt, därmed säkra att det är fysiken som gör skillnad och inte metoden. Det andra målet var att undersöka den baryoniska fysiken, vilket är fysiken kring normal atomisk materia så som protoner och neutroner, i den specifika delen runt om många galaxer vid namn intra-halo regionen, som är den region där ljuset från stjärnorna i halon, som heter intra-halo ljuset, kommer ifrån. Fördelningen av dessa stjärnor är förväntade att bero på egenskaperna hos mörk materia, men de beror också på den baryoniska fysiken som användes. Detta är därmed delvis ett förberedande arbete för att i framtiden undersöka hur en ändring på den mörka materians egenskaper har på detta intra-halo ljus, men för att göra det så måste man veta hur den baryoniska fysiken också påverkar det, så man kan sära på dem.

Popular Summary

The Universe is a strange place that has asked many questions, we have answered some of them but many remain and even more are unknown. One of those we have actively begun to answer is the question of dark matter. How do we know it exists? How can we learn more? What is it? The first of these subquestions has already been answered. We know mark matter exists because some unknown invisible mass is required e.g. for the rotational velocities of matter around galaxies, such as our own Milky Way, to make sense and for the massive structures we observe, such as galaxies and galaxy clusters, to be stable. But to understand these phenomena we need to know more about dark matter, and as it seems to have a large role for galaxies the answer might lie in their formation and evolution.

But the question is then, how can we learn more? One of the problems with learning more about dark matter is that we have made many different theoretical models but we can not test them experimentally, as many other branches of physics can, and instead rely on observations and computational methods. Observations are however for the most part out of the questions as they are very limited both due to our current technology but also because we only see galaxies at one of their many phases. We have therefore turned towards computational methods, more specifically simulations.

This work focuses on using these galaxy simulations, more specifically galaxies similar to the Milky Way, and their evolution with the purpose of analysing the properties of its gas, stars, and dark matter inside its bulge, disc, and halo. This was done firstly to compare with the results from the group researchers that gave the data called the AGORA (Assembling Galaxies Of Resolved Astronomy) Collaboration. They focus on verifying that the computational methods that are being used for the simulation codes produce the same results independent on the approach, therefore ensuring that the physics make the difference and not the method. The other goal was to analyse the baryonic physics, meaning the physics involving normal atomic matter such as proton and neutrons, in the specific part surrounding many galaxies called the intra-halo light, which is the light the stars in the halo produce. The distribution of these stars are expected to depend on the properties of dark matter, but also the baryonic physics that is being considered. This was partly a preparatory work to in the future analyse how a change in the properties of dark matter changes the intra-halo light, but for this to be possible one must know how the baryonic physics also affects it, so they can be separated.

Contents

Abbreviations and Acronyms

- CDM : Cold dark matter
- MW : Milky Way
- ESA : European Space Agency
- IHL : Intra-halo light
- IHR : Intra-halo region
- WIMPS : Weakly interacting massive particles
- AGORA : Assembling Galaxies Of Resolved Anatomy
- MUSIC : Multi-scale initial conditions
- UV : Ultraviolet
- IMF : Initial mass function
- Cal-4 : Calibration-4
- AMR : Adaptive mesh refinement
- SPH : Smoothed particle hydrodynamics

1 Introduction

Over the course of human history we have managed to explain many of nature's mysteries, but some remain elusive and understanding them gets more and more complicated. One of nature's strangest secrets is dark matter, a hidden presence throughout the Universe that carries mass and interacts, it seems, exclusively through gravitational effects and is vital for the formation and evolution of galaxies (Misiaszek and Rossi [2023]). In the pursuit to uncover the physics behind dark matter many hypotheses have been proposed of its properties, most notably its thermal velocity. The three main contestants, referred to as the "flavors" of dark matter, are "hot", meaning relativistic velocities, "cold", meaning non-relativistic velocities, and the intermediate "warm", which is somewhere in between (Arbey and Mahmoudi [2021]). Each of these have been tried in simulations but problems have risen for each.

To start, the hot dark matter models generated galaxies structures unlike those that are observed and the warm dark matter models have shown promise but are still fairly disputed (Schneider et al. [2014]). The cold dark matter (CDM) model, however, generally agrees with cosmological observations of large-scale structures such as galaxies and galaxy clusters but despite being well-received by astrophysicists, it faces numerous challenges many of which originating from the inconsistency between observation and simulation on smaller scales (Weinberg et al. [2015]).

1.1 Brief history of dark matter and the cold dark matter discrepancy

Dark matter is a fairly recent topic of debate, being only properly recognized as a problem in the 1970's when enough proof had piled up and the mysterious non-luminous matter quickly became a popular issue in several fields of science but mostly in astrophysics, cosmology and eventually particle physics (de Swart et al. [2017]). Before the 1970's, the concept of an invisible mass that seemingly had a very significant impact was initially quite controversial. The scientific community at the time believed that it would imply that the theories of astronomy were limited to less than 1% of all the matter that truly is, we now believe that normal matter contributes roughly 15% of all matter (Arbey and Mahmoudi [2021]). Instead it would be much more convenient to find a different explanation that fit better with their views.

The first proof that initiated the dark matter problem was the observational discrepancy in galaxy clusters, where it was found that for the gravitationally bound system to be stable there had to be a higher average mass density than what was seen van den Bergh [1961]. This was repeated with several clusters and the same discrepancy was found in each, leading to the hypothesis of dark matter. The second proof came a bit later, and caused the acceptance of dark matter, when it was found that the rotational curves of spiral galaxies were surprisingly flat, a very unexpected result from a seemingly Keplerian system Freese [2009]. For this to be possible there had to be some other significant mass that wasn't observed. Combining these two unconnected sources of proof provided the unequivocal evidence that was needed for dark matter to be taken seriously.

Assuming dark matter exists, as the evidence implies, the question then becomes what understanding it would imply for science and the scientific community. The obvious victor in such a discovery would be astronomy, especially cosmology. Dark matter seems to be a very important building block behind the Universe's large-scale structures such as galaxies and galaxy clusters and it would shed much light onto the understanding of their formation and evolution. Moreover, it also seems to have played a major role in the development of the early Universe via e.g. phase transitions, again mentioned by Arbey and Mahmoudi [2021]. They go on to state that an other field that would also benefit greatly is particle physics. As of now, the standard model does not include dark matter and thus if it were to be properly understood, a new model would have to be constructed to include it and its properties which might lead to many more discoveries.

What is currently found in the recent simulations assuming cold dark matter, using the properties that we believe it should have, is that the theoretically calculated gravitational lensing that the simulations give is much less effective than what is observed in from galaxies and galaxy clusters (Meneghetti et al. [2020]). The reason for this discrepancy is not completely understood but some astrophysicists today suggest that it must be either systematic issues with the current models or an incorrect assumption about cold dark matter's properties.

1.2 Disc galaxies and their structure

While galaxies can take many shapes during their formation, the important type for this thesis are the disc galaxies. Disc galaxies are defined, as the name suggests, as the galaxies with a flattened concentration of stars orbiting the galactic centre along the same plane (Jones et al. [2015], p.56-57). An example of a disc galaxy is our own spiral galaxy the Milky Way (MW) (see Figure 1), which was a focus in this thesis as the galaxies that were analysed had the same mass as the MW, and thus were called MW-like as they can be expected to have a similar general structure.

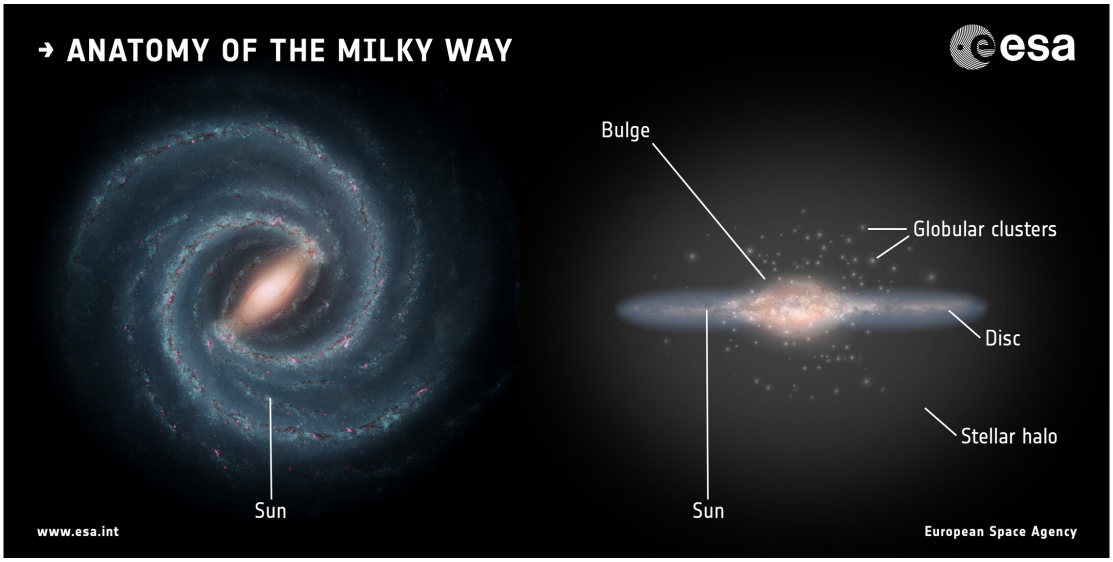

Figure 1: An artistic depiction of the Milky Way, both face-on and edge-on, and indicators pointing out its galactic components and the position of the Sun. Credit: ESA.

MW-like galaxies have, in addition to a disc, also a bulge, an inner both rotational centre and barycentre of densely packed older and metal-rich stars with a wide range of rotational velocities. While the disc and the bulge will be referred to as the two main components of the MW-like galaxies, the more important region for this thesis will be the remaining matter confined around these two components named the galactic halo. The galactic halo can be divided into three regions namely the stellar halo, which contains the stars, the galactic corona, which contains the hot gas, and finally the dark matter halo, which contains the dark matter. The region in focus in this thesis is the stellar halo, as the stars within this region will contribute to the so called intra-halo light (IHL), see later section 2.3.

1.3 Thesis goal and its structure

Many possible solutions to the CDM discrepancies have been proposed, such as modifying it with the previously mentioned warm dark matter models, changing the dark matter species where two main candidates are the Weakly Interacting Massive Particles (WIMPS) and the axions, or by studying and changing the baryonic physics as it will effect the dark matter distribution and the dark matter halo (Xu [2023]; Chan et al. [2015]). Depending on the chosen solution, it will have a noticeable effect on the distribution of stars in the stellar halo which can be analysed by looking at the resulting intra-halo light.

The main purpose of this thesis was to analyse and compare various cosmological simulations of the formation of MW-mass galaxies and study the influence of baryonic physics on the distribution of gas, stars, and dark matter in the intra-halo region. This was done, in part, to later in future work decouple it when studying different dark matter flavours. As we understand it, the choice of dark matter flavour should change the behaviour of galaxies' surrounding dark matter and their distribution of stars but to what degree and how it relates to observations is still a mystery.

The remainder of this thesis is structured as follows. Section 2 presents the necessary theory for this thesis such as the theoretical model used in the simulations and the simulation codes themselves together with their relevant physics. Section 3 describes some of the more specific methods used to get the results, for example, how the intra-halo region was isolated. Section 4 contains the final results the analysis of these results. Section 5 analyses and compares these results both with each other but also with results from the AGORA papers. Finally, Section 6 concludes the thesis and offers an outlook for further work.

2 Theory

2.1 The need for simulation and the AGORA collaboration

Theoretical models on these galactic scales can not be tested by observational or experimental methods but instead rely on simulations to thoroughly explore the impact of different dark matter considerations on the formation, evolution and properties of galaxies (MPG). All of these simulations are based on similar principles by first considering and basing the evolution of the galaxy around a certain cosmological model which are then allowed to, depending on the chosen initial conditions such as mass, metallicity etc., evolve via gravitational and baryonic interactions. The difference between the simulations are therefore which cosmological model that was chosen, the initial conditions of the galaxy, and which baryonic physics were considered and how they were implemented.

Even though current research in this subject of galaxy formation and evolution is dependent on simulations, there are relatively few groups of researchers that compare the effects of these simulation differences on the properties of galaxies. One of these groups is the AGORA collaboration, which has produced and compared several simulations of MW-like galaxies using similar, but differently implemented, baryonic physics (Kim et al. [2014]).

The cosmological simulations used in this report were generated by the AGORA (Assembling Galaxies Of Resolved Astronomy) Collaboration which aims to compare galaxy-scale numerical experiments using different implementations (AGORA). Their goal is to ensure that galaxy formation and evolution simulations succeed not because of the particular implementation technique but rather the physical considerations. As of now, the AGORA Project has over 160 participants across 60 institutions worldwide and together have published a total of 6 papers. These paper will throughout this thesis be referenced often and therefore, for convenience, they will from now on be referred to as Paper I (Kim et al. [2014]), Paper II (Kim et al. [2016]), Paper III (Roca-Fàbrega et al. [2021]), Paper IV (Roca-Fàbrega et al. [2024]), Paper V (Jung et al. [2024]), and finally Paper VI (Strawn et al. [2024]).

2.2 Models and the physics used by AGORA

Cosmological Model

The common and fundamental model which the simulated Milky Way-like galaxies were based on was the flat Λ-CDM cosmological model, known as the standard model of Big Bang cosmology (Scott [2018]), with a matter density of $\Omega_m = 0.272$, a vacuum density of $\Omega_\Lambda = 0.728$, and a Hubble constant of $H_0 = 70.2$ km s^{-1} (for more details see Paper III). This model assumes that cold dark matter has a significant role in the structure and evolution of galaxies, in the form of dark matter haloes, and that galaxies form and grow in a hierarchical manner by accreting and destroying lower-mass galaxies. This amassing of mass is not just from stars, gas, and dust but also from the dark matter contained in these smaller galaxies' dark matter haloes, now instead contributing to the dominating dark matter halo of the main galaxy. It is therefore expected to find a substructure of smaller dark matter haloes inside the main dark matter halo as they remain correlated despite their capture. A depiction of the evolution of the Universe according to this model can be seen in Figure 2.

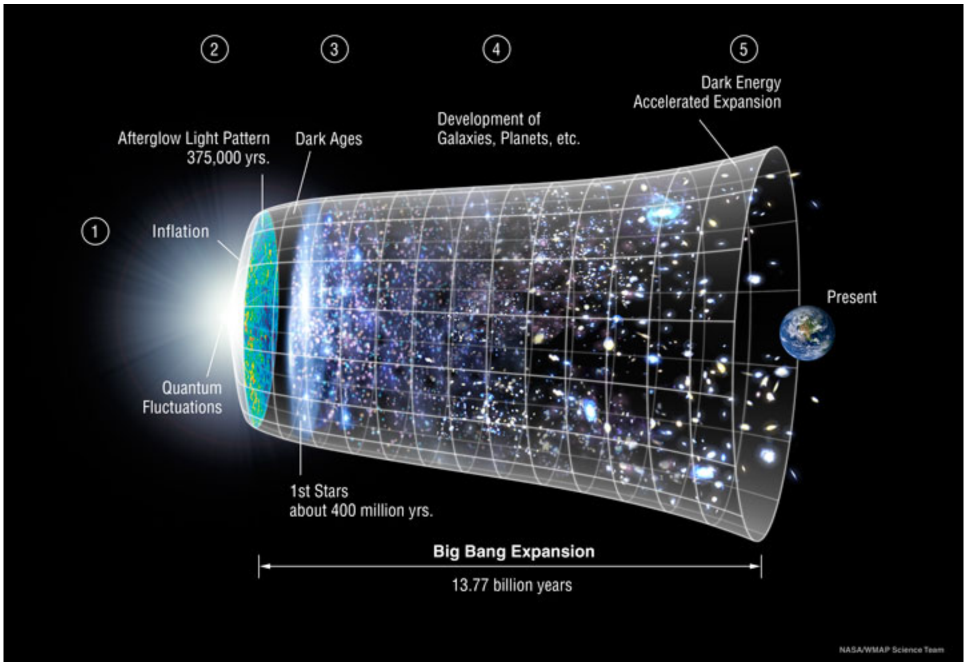

Figure 2: The evolution of the Universe, assuming the Λ-CDM model (credit: NASA/LAMBDAArchive/WMAPScienceTeam)

Common physics in the codes

When simulating any physical system it must be decided on which physics will be considered, obviously prioritizing the significant ones. But in some cases, such as when simulating galaxies, there are an incredible amount of possible considerations and it becomes difficult to gauge the importance of each of these, and choosing which ones, and moreover how they themselves should be implemented, requires significant planning and effort. To properly compare these codes, they must all be based on sufficiently similar physics to produce similar results but due to their different approaches this is not always possible.

The Milky-Way like galaxy simulations were taken at redshift $z = 4$ from the fourth calibration run, called Cal-4, of Paper III. The initial conditions were generated using MUSIC, which is an adaptive multigrid Poisson solver, assuming a flat Λ-CDM model and with the final halo virial mass of $\sim 10^{12}$ $M_\odot$ at $z = 0$. A short summary of the common physical considerations is the following:

- Radiative gas cooling: Metal-dependent cooling of the gas via radiation implemented using the GRACKLE library which uses a precomputed CLOUDY cooling table (Ferland et al. [2013]).
- UV background: Redshift-dependent ultraviolet radiation originating from the metagalaxy i.e. the total system of galaxies from GRACKLE (Haardt and Madau [2012]).

- Star formation: If an area of gas exceeded a density of $n_{\mathrm{H,thres}} = 1\ \mathrm{cm}^{-3}$, stars began forming at a rate of $\mathrm{d}\rho_*/\mathrm{d}t = \epsilon_* \rho_{\mathrm{gas}}/t_{\mathrm{ff}}$, where $\epsilon_* = 0.01$ was the formation efficiency and t_{ff} was the local freefall time.

- Supernova feedback: After a certain amount of time, depending on e.g. stellar mass, stars will evolve and eject metals and energy back into their surroundings. Depending on the code this was implemented differently, see the next section for more details.

- Stellar IMF and lifetimes: The distribution of stellar mass within a population was determined by the Initial Mass Function (IMF) presented in Chabrier [2003] and their lifetimes were determined from their mass and metallicity.

An important note is that although each of these physical considerations were included, they were not all implemented in the same way in each code. For further details and some of the more specific considerations see Paper I, II, and III.

Simulation codes and the code-dependent features

The astrophysical simulation codes providing the different Milky-Way like galaxies in this paper were ART-I, CHANGA, ENZO, GADGET-3, GEAR, GIZMO, and finally AREPO. This will provide a brief overview of their feedback techniques and their other distinguishing properties. Interested readers can read about further, more in depth details, in Paper VI.
An important difference between the codes was which feedback technique they each used as this will have a significant effect on, among other things, the total gas mass, the gas metallicity distribution and the stellar formation efficiency. The codes used collectively five different feedback types namely, thermal feedback, kinetic feedback, radiation pressure, delayed cooling, and finally superbubble. In Cal-4, each coding group within the AGORA Collaboration had the freedom to choose their favorite feedback schemes, meaning how the feedback is deposited, but they were restrained to always return 14.8 $\mathrm{M}_\odot$ of gas and 2.6 $\mathrm{M}_\odot$ of metal. The chosen deposited thermal energy and effective metal yields that were used for the simulations in this paper are included below. The effective metal yield was defined as how efficiently the surrounding gas was enriched by metals i.e.

$$\text{Effective Metal Yield} = \frac{m_{\mathrm{metals}}}{M_*}$$

where m_{metals} was the total returned metal mass and M_* was the total stellar mass.

ART-I is a Cartesian Adaptive Mesh Refinement (AMR)-type grid code originally from the paper by Kravtsov et al. [1997] and is based on an octree method where whenever a cell reaches a certain overdensity, in this case 4.0, they split in half in the three directions. It used thermal feedback, kinetic feedback and radiation pressure with a thermal energy release of $2 \cdot 10^{51}$ ergs per supernova and an effective metal yield of 0.033.

ENZO is also an AMR-type grid code but differs due to its open-source development strategy and history described more in the paper by Bryan et al. [2014]. It used thermal feedback with a thermal energy release of $5 \cdot 10^{52}$ ergs per supernova and an effective metal yield of 0.032.

CHANGA is instead a particle SPH code, based on the previous code GASOLINE, where the interactions between particles are "smoothed" and approximated across the domain (Menon et al. [2014]). It used thermal feedback and superbubble with a thermal energy release of $5 \cdot 10^{51}$ ergs per supernova and an effective metal yield of 0.032.

GADGET-3, also called GADGET3-OSAKA, is also a particle SPH code where the gravitational interactions between particles are calculated using a tree-particle-mesh method (Bode and Ostriker [2003]) and was introduced by Aoyama et al. [2017]. It used thermal feedback, kinetic feedback, radiation pressure and delayed cooling with a thermal energy release of $4 \cdot 10^{49}$ ergs per supernova and an effective metal yield of 0.025.

GEAR is another SPH code introduced by Revaz and Jablonka [2012] and is based on a previous GADGET generation GADGET-2 but with e.g. improved SPH formulation (Hopkins [2013]) and with both individual and adaptive time steps during integration (Durier and Dalla Vecchia [2011]). It used thermal feedback and delayed cooling with a thermal energy release of $4.5 \cdot 10^{51}$ ergs per supernova and an effective metal yield of 0.024.

GIZMO is a mesh-free code descending from GADGET-3 with a volume partition scheme meaning that the particles are represented instead with smoothed cells (Hopkins [2015]). It used thermal feedback and kinetic feedback with a thermal energy release of $5 \cdot 10^{51}$ ergs per supernova and an effective metal yield of 0.033.

AREPO is a more recent addition to the AGORA simulation codes and is a mesh-based code using an unstructured moving mesh, avoiding many of the disadvantages with using SPH or AMR (Springel [2010]). It used thermal feedback with a thermal energy release of $2 \cdot 10^{52}$ ergs per supernova and an effective metal yield of 0.034.

2.3 Intra-Halo Light (IHL) and Intra-Halo Region (IHR)

The definition of the IHL is generally fairly vague but this paper used the one in Proctor et al. [2023], which defined it as the observable extended component left after galactic accretion events i.e. the stellar light that is not from any satellite or the main galactic structures such as the disc and bulge, see Figure 3. The IHL is also commonly referred to as a stellar halo in galactic scales or intra-cluster light in galaxy cluster scales, but to remain consistent, even though only galactic scales will be relevant, the region where it was relevant was called the intra-halo region (IHR) and the combined luminosity from the stars was called the IHL in this thesis. It is worth noting, however, that this work did not convert the stellar mass into luminosity as the comparisons would have been identical. If instead stellar age was considered this would no longer be true and differences would emerge.

The significance of the IHL is mostly due to the history it contains and the relations that can be made between the properties of its constituents and the structure and properties of the galaxy as a whole. It acts as a graveyard for the many accretion events that occurred during

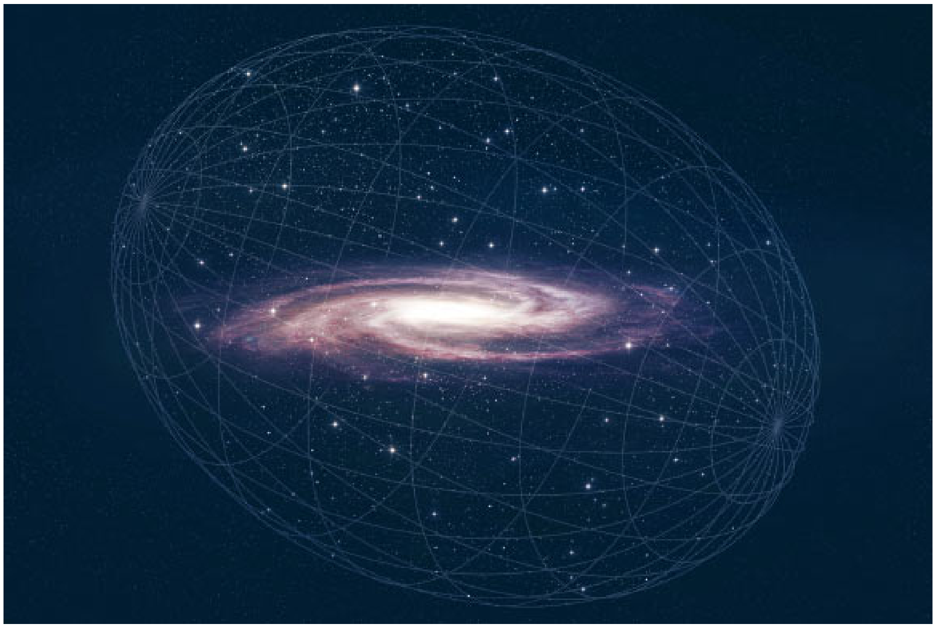

Figure 3: Artistic illustration of the MW stellar halo/IHR i.e. the stars that contribute to the IHL.
Credit: Melissa Weiss / Harvard & Smithsonian's Center for Astrophysics.

the evolution of the main galaxy with only the significant mergers, with larger galaxies containing many stars, remaining correlated for a longer duration in the form of stellar streams Deason and Belokurov [2024]. It can therefore be a very useful region to test physical considerations, such as baryonic physics or dark matter flavours, as changes in these are believed to have a noticeable impact on the behavior and properties of the IHL and its constituents.

3 Methodology

3.1 Analysis tools

The coding language used was Python version 3.12.1, and the primary tool used to load and manage the AGORA data from the galaxy simulations was `yt` version 4.0, a community-driven and developed toolkit for visualising and analysing quantitative data (Turk et al. [2010]). `yt` is the decided toolkit used by the AGORA Collaboration for their own analyses and comparisons. `yt` was used also in this paper to generate the radial profiles in the results section which were then plotted using `Matplotlib`. Additional tools for analysis and comparison were also `Numpy` and `SciPy`. Much of the code written and used to produce the results was heavily inspired by code written and provided by the AGORA Collaboration, but with some modifications to allow for analysis of specifically the IHL.

Reading and handling the data

All the Cal-4 data was downloaded via a provided cloud database and then loaded in via `yt`'s `load()` function. Each code had differently defined variables, such as the field type for gas, mass, and dark matter, and thus to keep it consistent, the data of each code was contained in a respective class simply called Code, where in the constructor each field type and field name, such as mass, metallicity etc., were defined with the same instance variable independent on the code. This made it a lot easier later in the code when the data had to be acquired via, for example, a `for` loop. Also, the centering of each code's galaxy were handled by simply defining another instance variable with the found and given location of the centers of each galaxy by AGORA.

One of the properties that had to be redefined was the metallicity, which in this case was measured using the metal abundance which is the total amount of metals compared to the hydrogen mass. This is not the same as metallicity, but will show the same effects when plotted and can more easily be compared with observations and henceforth the "metallicity" will be the abundance. The codes contained the metal mass and the total mass of each cell/particle in solar units which were then used to find their metal mass fractions Z/X which were equivalent to their number fraction N_Z/N_X. First, their metal mass fractions were divided by the solar metallicity of $Z_\odot \approx 0.0204$, to get the absolute values. Then, the abundance formula that defined the metallicity field was

$$A = 12 + \log_{10}(M/H),$$

where M was the total metal mass and H was the total mass for that cell/particle, 12 was added to make comparisons easier.

Then, the profiles were generated using the `yt` `create_profile()` function, with 50 bins and where the weight field was set as the mass field of the corresponding field type, to get a mean value, except for the mass profiles themselves that were unweighted as the total mass distribution was instead desired. These profiles were then plotted using `Matplotlib` with the same colour scheme found in the AGORA papers.

Isolating the IHR

To analyse just the cells/particles belonging to the intra-halo region, the other parts had to be removed from the data sets. There are many methods one could use to achieve this, such as filtering them based on chemistry, kinematics and/or age. The chosen method was by far the simplest, at least in theory, and involved just cutting spherical holes at the centres of the galaxy and the many satellites.

The radius of these holes, called the transition radius, were chosen to be a fraction of the virial radii $R_{\rm vir}$ of their respective component. The virial radius is defined as the radius of a spherical region within which the density is equal to or surpasses the critical density of the Universe, meaning the density where the Universe is at balance at that specific redshift and does not expand, allowing for the collapse into structures. The centres and the virial radii were all provided by AGORA who found them using the halo finder ROCKSTAR (Robust Overdensity Calculation using K-Space Topologically Adaptive Refinement) (Behroozi et al. [2012]). After testing and minimizing contamination from the main structures, the fractions of $R_{\rm vir}$ were chosen to be 0.25 for the main galaxy and 0.5 for the satellites, for an example see Figure 4.

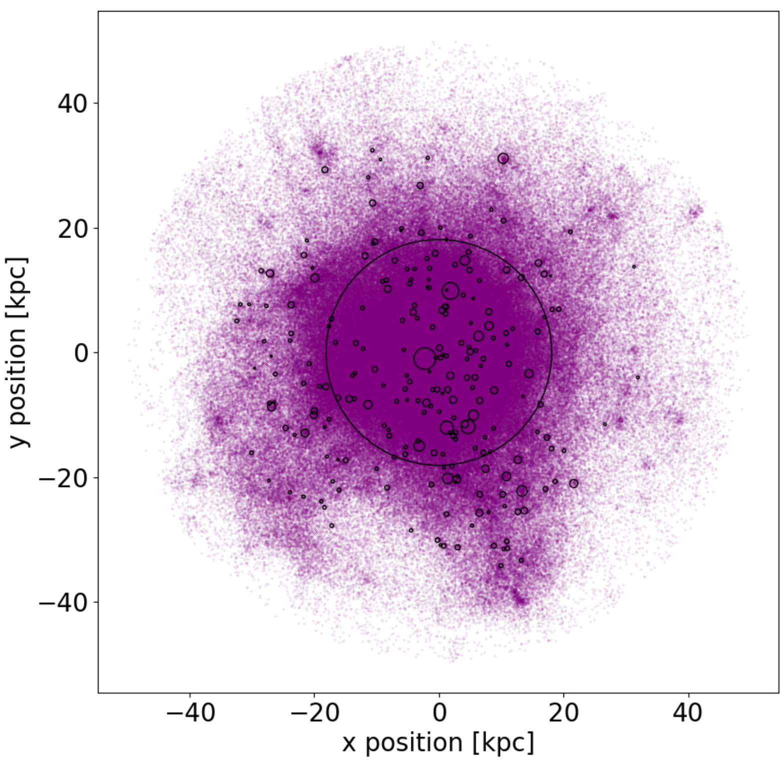

Figure 4: The dark matter x and y positions relative to the centre of the MW-like galaxy at redshift $z = 4$ produced by AREPO, together with black circles indicating the regions that were removed.

While the method of using a transition radius, i.e. a radius defining an edge between the intra-halo region and the rest, has been shown to be an ineffective way to define the intra-halo region at redshift $z = 0$ in e.g. Proctor et al. [2023], it can be justified by considering the scope and level of complexity possible for this work and it will suffice for these purposes. On the other hand, in the same paper they defined their transition radius very differently and as a result found that a majority of the components belonging to the IHR were inside the radius and thus removed. In this work, the transition radius was significantly smaller which most likely increased the contamination from the other components but at the same time most of the IHR would have been included.

Removing empty points and the bulge

During plotting it was found that some codes had bins/points in their IHR star profiles with the value of zero for every property at certain radii. This was not expected and most likely due to them having too few stars left in the IHR and these regions being simply empty. Keeping these points made comparisons much more difficult as they could not be logged and thus the plots where discontinuous along the radius. This was therefore circumvented by simply removing those points at the cost of resolution. Furthermore, close to bulge some fields had significantly higher values than the rest and thus the region $r < 0.2$ kpc had to be removed to get a more reasonable plotting range for the rest. As the bulge region was not the focus in this paper and was completely removed when isolating the IHR, this should not have had any significant effect on the comparisons.

4 Results

4.1 After isolating the IHR

The results of applying the method described in Section 3.1 for the stars is shown in Figure 5, and as can be seen most of the disc and bulge had been removed, leaving the diffuse stars surrounding them i.e. those who belonged to the IHR.

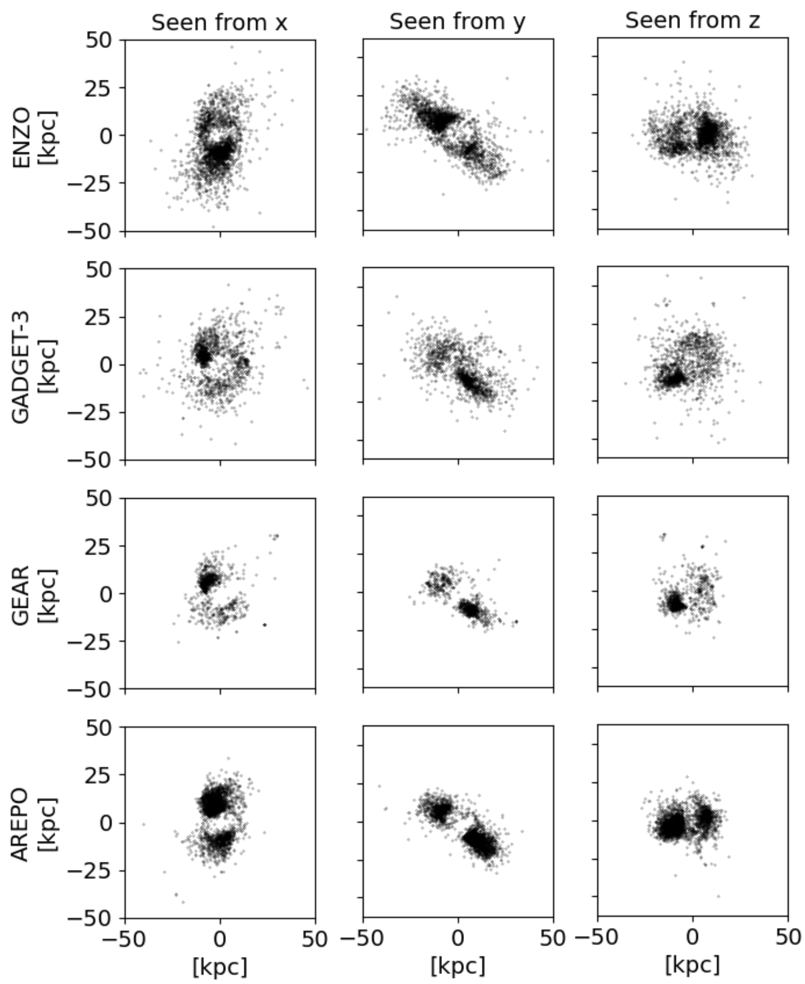

Figure 5: The star particles belonging to four of the codes (ENZO, GADGET-3, GEAR, and AREPO) after removing the satellites, disc, and bulge plotted along the three Cartesian axes.

Comparing the IHR star distribution in each galaxy from each code in Figure 5 showed a clear difference in both general shape and density. As stated in Paper III, these snapshots at redshift $z = 4$ captured the galaxies right after a merging event with another major galaxy. This could explain the asymmetrical shapes of many of these galaxies, especially AREPO, as their haloes have stabilized less than ENZO. They also continue by stating that using snapshots at these crucial redshifts, with high perturbation, should ideally be avoided and one must be careful when comparing any of the galaxies' properties. Another unfortunate consequence of this was that it seems as many of these codes still had much denser regions of stars that would not be expected for IHR stars, especially AREPO and ENZO.

The total fractions of the gas, stars, and dark matter and their mass that was removed can be seen in Table 1.

Table 1: The count and mass fractions of gas, stars, and dark matter that were removed from each simulation when isolating the IHR.

Code / Fraction:	N_{gas}	N_{star}	N_{DM}	M_{gas}	M_{star}	M_{DM}
ENZO	0.32	0.91	0.25	0.36	0.91	0.25
GADGET-3	0.34	0.99	0.24	0.35	0.99	0.24
GEAR	0.63	0.98	0.24	0.63	0.98	0.24
AREPO	0.36	0.86	0.24	0.37	0.86	0.24

This shows that a significant part of the stars were removed ($\approx 86 - 99\%$), while much less of the gas ($\approx 32 - 63\%$) and even less of the dark matter ($\approx 24 - 25\%$) was removed. This was reasonable as the regions with dense stellar populations were removed i.e. the disc, bulge and the satellites, and while the gas was more dense in these regions it was still much more spread out throughout the galaxy than the stars. The dark matter was shown to be even more spread out, and relatively unaffected, across the galaxy as the fraction of the dark matter that was removed was both much less and had a much more narrow range between codes than the gas and the stars.

4.2 Comparing Profile Plots

Gas component in the whole galaxy

Firstly, the gas properties in each of the codes' galaxy, both with and without disc/bulge/satellites were, radially profiled inside a 50 kpc sphere centred on their respective galactic centre, which was provided by the AGORA Collaboration, and then plotted in Figure 6.

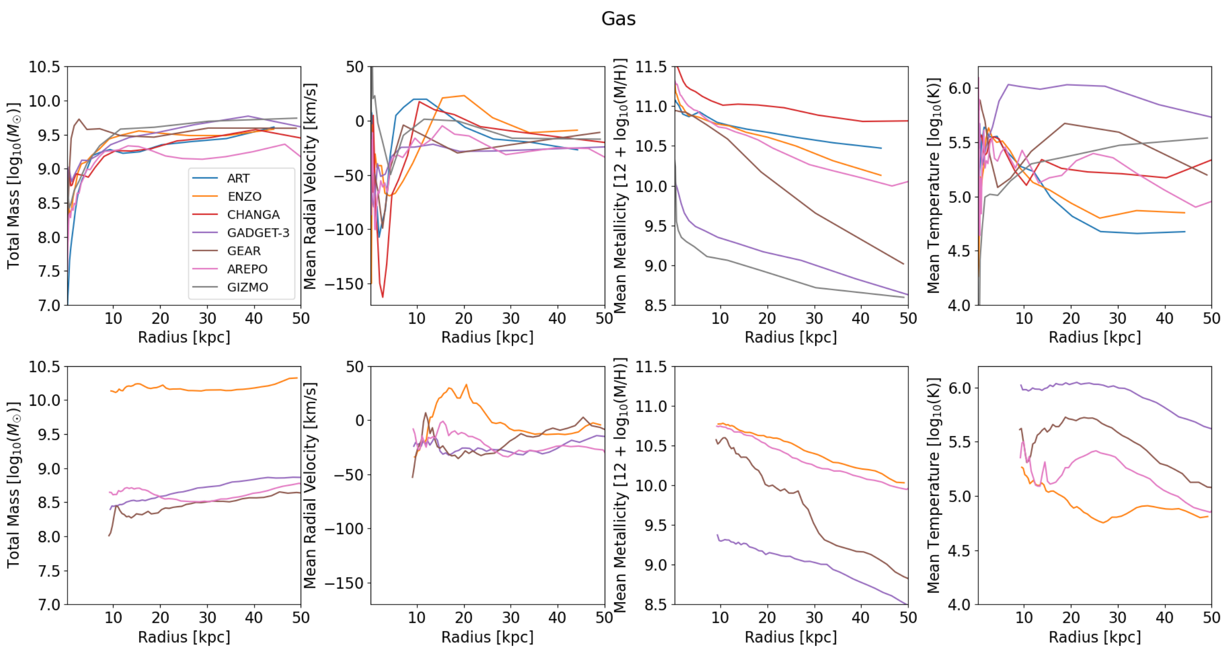

Figure 6: Radial profile plots of the four gas properties, mass, radial velocity, metal mass, and temperature, with colour indicating the code, considering the whole galaxy (first row) and in the codes with available satellite data considering only the IHR (second row). Note that all gas properties other than radial velocity were logged before plotting.

Starting with the plots of the whole galaxy, first row in Figure 6, showed overall a fairly good resemblance between the codes, mostly towards higher radii, as they all had similar behaviour and were not separated by more than half of a magnitude. Firstly, the mass plots, first row, first column, were seemingly very closely-knit and all stabilizing into a roughly constant value, with two notable outliers at certain radii. The first of these was that GEAR had a much higher gas mass closer to the centre, the second was AREPO, which at a higher radius deviates and had a slightly lower mass than the others.

Following the mass plots, the radial velocity plots, first row, second column, showed also a strong similarity between the codes with each having roughly the same shape. A notable difference was both that they each seem slightly shifted along the radius relative to each other at lower radii despite bunching together nearer the edge of the sphere. Also, the strength of their features, the initial dip into high negative velocity and the following bump back up was somewhat different between the codes, specifically CHANGA had a much higher dip near the centre inferring that it could have been a lot more heated and turbulent in this region.

The metallicity profiles, first row, third column, were divided into two main groups, firstly ART, ENZO, CHANGA, GEAR, and AREPO who all had a high metallicity at their respective bulge, with CHANGA dominating, unlike the second group with GADGET-3 and GIZMO that were significantly lower. The behaviour further out also differed quite a lot with CHANGA remaining very consistent and only slowly decreasing, ART, ENZO, and AREPO kept close together deviating after roughly 20 kpc, when ENZO and AREPO started decreasing more than ART. GEAR had a much steeper decline, rapidly dropping in metallicity in the galaxy's outer regions further than 10 kpc, which was roughly the cutoff when the IHR started. GADGET-3 and GIZMO with a similar behavior as ART, steadily decreased but now at a much lower metallicity.

The final plots for the gas in the entire galaxy were the temperature profiles, first row, last column, and as can be seen they were fairly different, differing not much more than one magnitude however. Close to the bulge most seemed to start at roughly the same magnitude of ~ 5.5, but in this region it was also very noisy. Further out GADGET-3 clearly dominated and peaks at a temperature of roughly 10^6 K at around 8 kpc, after which it steadily decreased. ART and ENZO seemed to stay close together showing similar behaviour at the lowest temperature, and GEAR and AREPO seemed to behave similarly but with different values.

Gas component in the IHR

On the second row, are instead the profiles belonging only to the IHR, with some notable features and differences. Unfortunately, the satellite data, i.e. their positions, virial radii etc., were only available for four of the codes, namely ENZO, GADGET-3, GEAR, and finally AREPO, meaning that there were not as many codes that could be compared. Regardless, comparing these plots overall showed similar trends as with the plots in the first row with fairly good resemblance, at least for the mass and radial velocity.

Looking closer at the total mass distributions, second row, first column, showed that three of the codes, GADGET-3, GEAR, and AREPO, were close relative to each other but with ENZO being an obvious outlier. The reason for this large deviation was unknown and probably a fault with plotting as this was not found in the AGORA papers III or IV. Suspected causes were either complications with `yt` when filtering the dataset, or a unit discrepancy. Unfortunately, due to lack of time, this could not be analysed in this thesis and will instead be left as a future endeavour.

Then, the mean radial velocities profiles for the gas in the IHR, second row, second column, had similar behavior but with ENZO initially deviating strongly within the 10-30 kpc region but eventually overlapping significantly with GEAR.

Comparing the gas metallicity plots, second row, third column, showed a strong similarity in behaviour between the codes, especially ENZO and AREPO who also shared similar values, where their metallicities, as expected, decreased with further out from the centre where there was weaker stellar formation and less contamination of the non-IHR gas.

Finally, the mean temperature profiles, second row, last column, had similar values as when considering the whole galaxy which could have meant that the gas inside the satellites at radii further out than $0.25\mathrm{R}_v$ were not significantly heated compared to the surrounding gas in the IHR.

Star component in the whole galaxy

As with the gas, the stars' properties in both the whole galaxy and the IHR were radially profiled in the same 50 kpc sphere and the results can be seen in Figure 7. Note that the temperature property is missing due to it not being available and as straight forward to determine as with the gas.

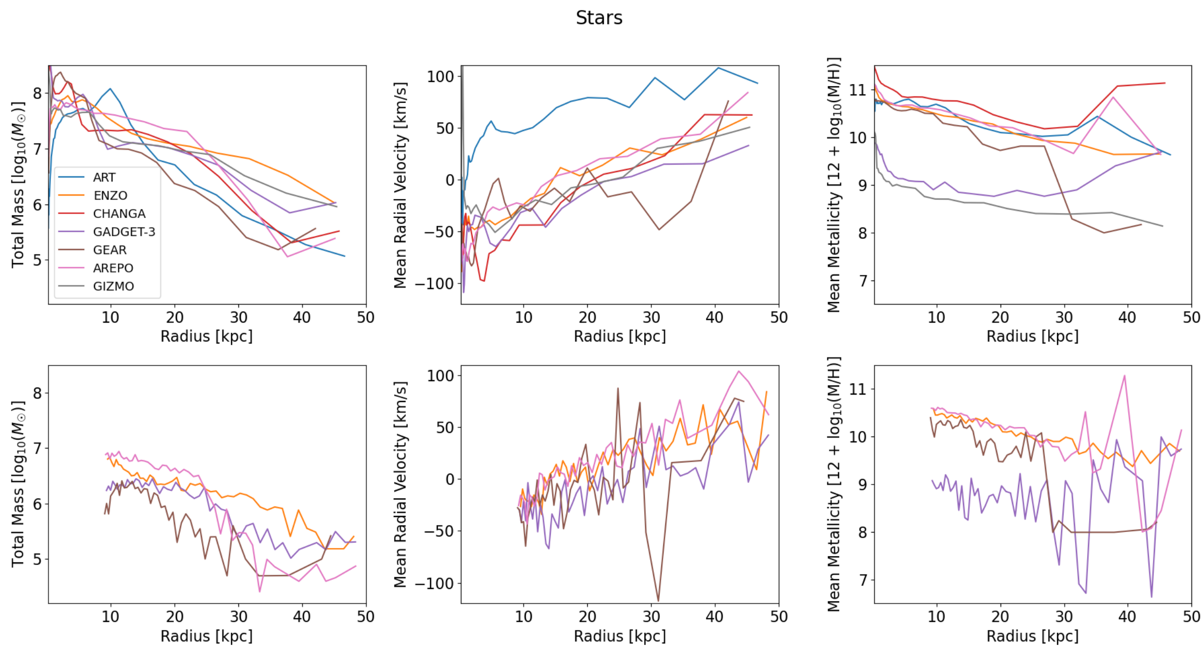

Figure 7: Radial profile plots of the three star properties, mass, radial velocity, and metal metallicity, with colour indicating the code, considering the whole galaxy (first row) and in the codes with available satellite data considering only the IHR (second row). Note that all star properties other than radial velocity were logged before plotting.

As before, firstly the whole galaxy were analysed and then the IHR. First of all, the mass plots of the stars, first row, first column, had similar behaviour between codes where they decreased seemingly linearly with radius, starting off fairly similar closer to the centre but deviating further out while still remaining within a range of about one magnitude between the codes.

The second plot was the average radial velocity profile of all stars within each galaxy, first row, second column. Most codes followed had a congruent negative mean radial velocity close to the bulge that, further out, increased in a linear fashion from negative to positive, experiencing an average of zero radial velocity in the range of 20-30 kpc from the centre. Two codes acted unlike the rest. The first of these two was ART, that seemed to have started roughly at a similar velocity like the rest but quickly deviated towards, and remained at, high positive radial velocity. The second outlier was GEAR, which mostly acted similar to the others until around 25 kpc, where most of the codes reached an equilibrium of radial velocities, where it instead had a sharp decrease to roughly -50 km/s. At roughly a distance of 35 kpc, it returned to the majority of the codes.

Finally, the last stellar radial profile in the whole galaxy was the mean metallicity, first row, last column. Comparing these metallicity profiles with those of the gas in the entire galaxy (see Figure 6) revealed a strong resemblance. In both profiles GADGET-3 and GIZMO, and ART and ENZO were paired together, CHANGA dominates, and GEAR had an obvious decreasing trend but in the star case much more rapidly. Unlike the gas profiles, however, GADGET-3 deviated from GIZMO and GEAR at a higher radius and overlapped instead with ART, ENZO, and AREPO.

Star component in the IHR

Moving on to the stellar component of the IHR, which was the part that was producing the IHL, firstly the mass profiles of each code, second row, first column, seemed to, except for a decrease of about one magnitude, not have changed in any obvious way. They were each still very clearly trending downwards with increasing radial distance. One thing worth noting was that GEAR seems to have had a stronger resemblance with the majority than when the whole galaxy was considered, leaving AREPO behind. Strangely during analysis of the stars in the IHR, for some reason certain points at higher radial distance, mostly around 30-40 kpc, had the value of zero, leading to an error when logging. This was circumvented by removing these points before plotting but this resulted in decreased resolution within these ranges. The reason for this was most likely due to the relatively few star particles further out so some bins could have been simply left empty. A clear example of this was GEAR, who had the most problems in the region after 30 kpc where less points were plotted compared to the other codes. But seeing as the IHR profiles had the same amount of total bins as the whole galaxy but are within a smaller range of radial distances as the inner most region was completely removed, some of the resolution was recovered.

The stellar radial velocity profiles for the stars in the IHR, second row, second column, had a similar general behavior as their counterpart in the whole galaxy where they were fairly congruent and from negative velocity linearly increased with radial distance. The clear difference was that the IHR stars were much more noisy with a significantly wider range of values.

The final profiles for the IHR stars were the metallicites, second row, last column. Overall similar behaviours as the corresponding whole galaxy profiles, with a few notable differences. The most significant one was the values as these have for all codes increased. This was an expected result as the stars in the IHR should have had a much higher metallicity. Then, as with the other IHR star profile plots, they were much more noisy as, among possibly other things, the sample size had dramatically decreased. Despite this, most codes seemed to near each other as before, except for GEAR.

Dark matter component in the whole galaxy

The third and final matter that was analysed was dark matter, which was as the two previous matter forms radially profiles in the same 50 kpc sphere and the results can be found in Figure 8. Note that the only relevant properties of dark matter was the total mass distribution and the radial velocity, as dark matter is neither made of baryonic matter, i.e. no metallicity, nor interacts electromagnetically.

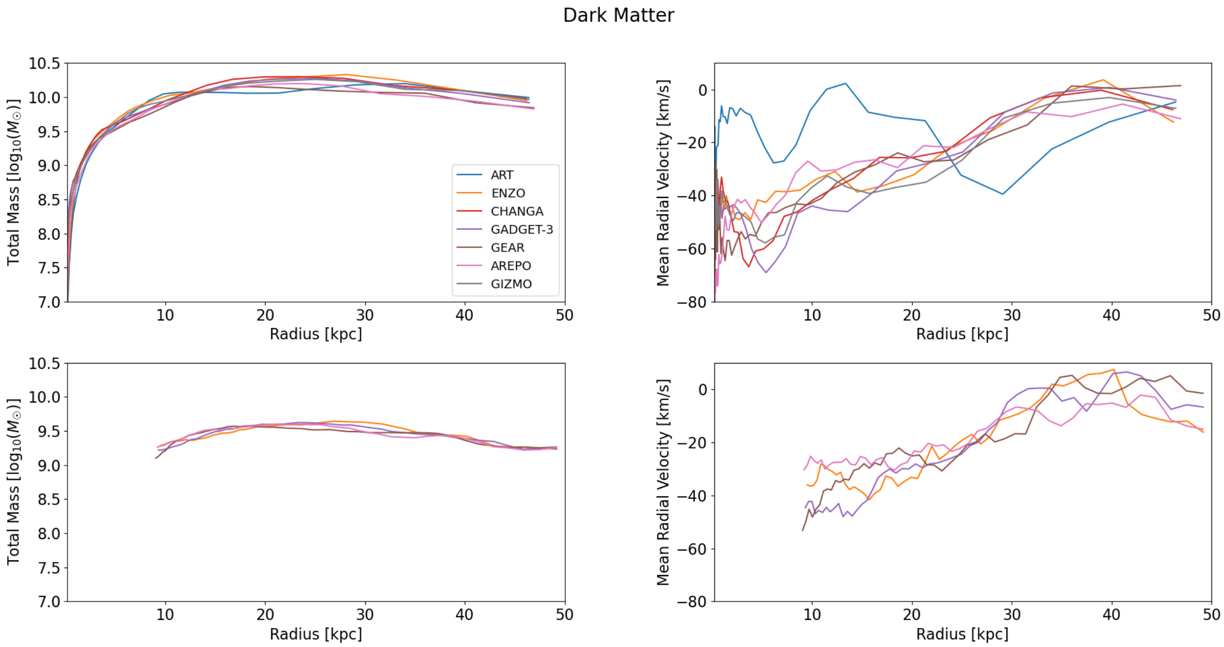

Figure 8: Radial profile plots of the two dark matter properties, mass, and radial velocity, with colour indicating the code, considering the whole galaxy (first row) and in the codes with available satellite data considering only the IHR (second row). Note that all dark matter properties other than radial velocity were logged before plotting.

The radial total dark matter mass distributions in the whole galaxy, first row, first column, were highly similar, nearly indistinguishable, throughout the entire 50 kpc range. This was expected as it was already been hinted at from the previous result that showed that the removed dark matter fraction (both mass and count) range between codes was relatively narrow compared to the other matter types. The common curve that all profiles resembled at lower radii ($\lesssim$ 20 kpc) was that of logarithm growth, followed by a roughly constant value at $\sim 10^{10}$ $M_{\odot}$.

Moving on to the mean dark matter radial velocity profiles in the whole galaxy, first row, last column, showed also very similar and overlapping curves from the majority of the codes, especially at higher radii ($r > 25$ kpc). As with the stars, ART stuck out and acted unlike any of the other codes, being seemingly shifted upwards and having a much lower negative radial velocity closer to the bulge with no clear trend until around 30 kpc where it steadily increased and neared the other codes.

Dark matter component in the IHR

Very similar in behaviour as the whole galaxy, the total dark matter mass in only the IHR, second row, first column, seemed to just decrease, as was expected from previous results. Additionally, it can be seen that the similarity between codes seem to have been even better, especially between ENZO and AREPO, and at the edge of the 50 kpc sphere they seem to have almost completely overlapped.

The final profile plot to be analysed was the mean radial velocity for the dark matter in the IHR, second row, last column. Initially each profile behaved very similarly to its counterpart in the whole galaxy but after roughly 20 kpc, some of them, such as GADGET-3, started behaving much more erratically and no longer smoothed out further away from the center but rather went up and down. In addition, it seemed like the profiles were more spread out than in the whole galaxy but they do seem to have gathered together at the edge in a very similar way.

5 Discussion

The results from isolating the IHR showed that the chosen method was, as suspected, not perfect as the IHR should have been a diffuse region of stars but yet several dense regions of stars remained. This could have been from forgotten satellites or remnants from the merging event that did not belong in the IHR. On the other hand, it was shown that a vast majority of the stars were removed, between 86% to 99%, meaning that these seemingly dense stellar regions that Figure 5 showed might not have been as problematic as believed, or perhaps many of the IHR stars were accidentally removed. A more proper method of isolating the IHR would have made it much easier to discern which of these were correct. Possible methods could have been to use the techniques presented in Proctor et al. [2023]. One of these would have identified the IHR based on the ratio between the specific angular momentum along the z-direction and the specific angular momentum of a particle with the same binding energy on a circular orbit. Another instead found the IHR by using the ratio between the specific binding energy of a particle to the minimum specific binding energy, i.e. the most bound particle, in the galaxy. Other methods could be to use those shown in Veljanoski et al. [2018] where they developed a machine learning model to find the stars belonging to the IHR via their distinguishing properties. Unfortunately, all of these options were way beyond the scope of this thesis.

In Proctor et al. [2023] they found the stars in the IHR mass fraction $f_{*,\text{ IHR, proctor}} \approx 0.08$ for MW-like galaxies which was not too far off from the values found here (0.01 - 0.14) and was quite similar to the average between the different simulations of $\langle f_{*,\text{ IHR}} \rangle \approx 0.065$. However, a very important difference was that the Proctor paper used Milky Way-like galaxies at redshift $z = 0$, which was expected to result in a different stellar distribution as there would be more time for e.g. merging events, and stellar formation. How successful this method is for lower redshift could be something done in a future work, where also a recent merging event can be avoided.

Comparing the fractions in Table 1 between the codes revealed a couple of differences. For starters, GEAR deviated strongly from the rest with how much of the gas that was removed, revealing that its galaxy could have had a much higher gas density in the stellar regions. This was consistent with the results from Paper III which found that GEAR had an accumulation of dense warm-hot gas in star-forming regions, which would be closer to the satellites and the disc/bulge. Additionally, ENZO and more so AREPO seems to have had slightly more stars in the IHR than the others meaning that their galaxies would have had a brighter IHL. Both of these results were later further supported by the profiles plots as the total mass distribution of the GEAR code showed a much higher gas mass closer to the centre, and initially the total star mass were dominated by ENZO and AREPO up until around 28 kpc, where AREPO decreased. The reason for this sharp decrease in star mass could be due to remnants of non-IHR stars, that would be more massive as they were from high star forming regions, that were incorrectly included. AREPO did have the highest fraction of stars in the IHR and from Figure 5 it seemed like AREPO had, among the codes, the most dense regions of stars remaining. What Proctor et al. [2023] also found was that at around $r \approx 30$ kpc, the IHR starts to dominate the stellar mass distribution which could explain the decrease at around that radius as further out than that any contamination from non-IHR stars might not have been as significant.

The profiles plots for the total mass and the mean radial velocity of the gas, stars, and dark matter in the whole galaxy revealed a reoccurring pattern of both similar behaviour and fairly strong similarity between most codes (within half a magnitude), which corresponded well with the results from the AGORA papers, especially Paper III. There were, however, some notable exceptions where this did not hold both for the gas in the IHR of the ENZO simulation and for the stars and dark matter in the whole galaxy of the ART simulation. In the first case it was, as previously mentioned, most likely an incorrect result and caused when filtering the dataset using `yt` as it was not found in any of the AGORA papers. Due to ENZO being an AMR code, the filtering when isolating the IHR had to be treated differently and thus as ENZO was the only code in the IHR that acted this way, it could have been the problem. Strangely, however, the behaviour of ENZO's IHR profiles in the other gas properties and the other matter forms, i.e. stars and dark matter, did not have this strong deviation, which instead supports the unit discrepancy explanation. Unfortunately, the true answer is left unknown due to limited time but could be revisited in a future work.

Another likeness to the AGORA papers, especially Paper IV, that was found was that the metallicities of both the gas and stars had a much wider range, with less similarity, than the other properties. This made sense as the metallicity depended strongly on the chosen feedback parameters and scheme, as stronger feedback would scatter the metals more and the mean metallicity can be expected to be less. As each of these codes had different feedbacks, they were expected to have quite different metallicity profiles, but codes with more similar feedbacks, such as firstly ART, ENZO, and AREPO, and secondly GADGET-3 and GIZMO had very similar behavior. Unfortunately, the IHR in the ART and GIZMO simulations could not be studied as the data for their satellites' centres and virial radii were missing but ENZO and AREPO kept strong similarity in the IHR as well, most likely due to their similar strategy of high ($\geqslant 10^{52}$ ergs per supernova) and pure thermal supernova feedback.

Comparing the profiles of the whole galaxy with the corresponding profiles of only the IHR showed that in almost every case the behaviour was the roughly the same, especially for the dark matter, and for the total mass distributions the values also, as expected, decreased as much of the mass was removed. The only noticeable difference was an increase in noise which was probably due to both the amount of bins per kpc had increased but also because the sample size decreased, very significantly for the stars. Another possible explanation, at least for the mean radial velocities, could be that it was an expected behaviour of the IHR, as it has been observed that the IHR is more spherical in shape which would only be possible if the radial velocities had a much wider, almost random, range.

These results showed, as was also shown in Paper IV, that using different supernovae feedback schemes will have a significant impact on the metal abundance in the gas and stars in the galaxy but not nearly as much on their total mass distribution or their mean radial velocities. Therefore, changing assumptions in the model, more specifically the dark matter flavor, would then be directly noticeable as these changes are expected to have a much more significant effect on the total mass distribution and mean radial velocities. Knowing the smaller impact on these two properties from the baryonic differences makes it possible to decouple it from the differences from changing the dark matter flavor and then analyse those more thoroughly.

6 Conclusion and Future Work

To conclude, this thesis was an example of a code comparison project where gas, star, and dark matter properties from Milky Way-like, cosmological, and hydrodynamical simulations produced by different codes, with various computational methods and slightly different baryonic physics, were compared between each other. This was done in order to both compare with the AGORA code comparison papers, that used the same or similar data, to verify the reproducibility but also to extend into studying the specific galactic component called the intra-halo region (IHR) which is the matter outside the disc and bulge where the intra-halo light (IHL), i.e. the stellar luminosity from the stellar halo, can be discerned, and try to unveil the consequences of differences in baryonic physics.

The method chosen for isolating the IHR, i.e. removing the main galactic components, was found to be fairly effective in removing significant amounts of the non-IHR matter but not very accurate, as clumps of probably mostly non-IHR matter remained, in some codes more than others. The total mass and mean radial velocity profile plots of each matter type, gas, stars, and dark matter, in the whole galaxy revealed a common trend of strong congruence between the codes, verifying the behaviour found in the AGORA papers, especially for the dark matter. It was also found that, as expected, the profiles that were most dissimilar were those where feedback mattered most, the mean metallicity and temperature, and this was also found in AGORA's Paper III and IV.

When comparing the IHR properties with those of the whole galaxy it revealed a very strong similarity in both behaviour and for the mean properties also value, the total mass obviously decreased as mass was removed. The significant difference was the amount of noise and the broadening of the curves, this could be ascribed to either the loss of sample size when removing much of the mass, probable for the stars as they were not many left, but alternatively there is also observational evidence that the participating matter in the IHR, such as the stars, has a much wider range of, for example, radial velocities as the IHR is generally observed to be spherical in shape.

A clear improvement for this thesis would have been to include more codes where the IHR could be isolated. While four codes were by no means too few, some codes, such as ART, had interesting behaviour in the whole galaxy and it might have been useful to see if it was replicated in the IHR as well. This could have been done together with another possible improvement which would have been to define the IHR with something more or else entirely than just a transition radius. The chosen method made it was hard to know whether the behaviour of the IHR profile plots were influenced by non-IHR particles or not. While it was clearly shown that much of the gas, stars, and dark matter was removed, it would be more accurate to instead define the IHR by its known observational properties, such as its kinematics, via the methods used by other papers mentioned in Section 5.

While these results are not suitable to be compared with observations, as the differences in observable properties, such as metallicity, are too spread out and inconsistent between codes to produce any reasonable conclusions. They could, however, be used to improve the model and parameters to work towards more closely resembling observations.

The goal of this thesis was initially to instead analyse the effect of different dark matter flavours at different redshifts on the IHR but unfortunately the simulations that were going to be used were not developed in time and this is instead left as a possible future endeavour. Therefore, more focus had to be placed on the available data and therefore the baryonic physics of IHR. These results could perhaps be used in this future work as changing the dark matter flavor is expected to have a much more noticeable effect, compared to different baryonic physics, on the total mass distribution and the radial velocities. This work ensured that the codes had strong similarity in these properties, in both the whole galaxy but also in the IHR, despite different baryonic physics, making it possible to compare and decouple them from the effects of using a different dark matter flavor.

References

Marcin Misiaszek and Nicola Rossi. Direct detection of dark matter: a critical review, 2023.

A. Arbey and F. Mahmoudi. Dark matter and the early universe: A review. *Progress in Particle and Nuclear Physics*, 119:103865, July 2021. ISSN 0146-6410. doi: 10.1016/j.ppnp.2021.103865. URL `http://dx.doi.org/10.1016/j.ppnp.2021.103865`.

Aurel Schneider, Donnino Anderhalden, Andrea V. Macciò, and Jürg Diemand. Warm dark matter does not do better than cold dark matter in solving small-scale inconsistencies. *Monthly Notices of the Royal Astronomical Society: Letters*, 441(1):L6–L10, March 2014. ISSN 1745-3925. doi: 10.1093/mnrasl/slu034. URL `http://dx.doi.org/10.1093/mnrasl/slu034`.

David H. Weinberg, James S. Bullock, Fabio Governato, Rachel Kuzio de Naray, and Annika H. G. Peter. Cold dark matter: Controversies on small scales. *Proceedings of the National Academy of Sciences*, 112(40):12249–12255, February 2015. ISSN 1091-6490. doi: 10.1073/pnas.1308716112. URL `http://dx.doi.org/10.1073/pnas.1308716112`.

J. G. de Swart, G. Bertone, and J. van Dongen. How dark matter came to matter (vol 1, 0059, 2017). *NATURE ASTRONOMY*, 1(4):0090, 2017. ISSN 23973366. URL `https://ludwig.lub.lu.se/login?url=https://search.ebscohost.com/login.aspx?direct=true&AuthType=ip,uid&db=edswsc&AN=000406533900012&site=eds-live&scope=site`.

Sidney van den Bergh. The stability of clusters of galaxies. , 66:566, December 1961. doi: 10.1086/108466.

K. Freese. Review of observational evidence for dark matter in the universe and in upcoming searches for dark stars. *EAS Publications Series*, 36:113–126, 2009. ISSN 1638-1963. doi: 10.1051/eas/0936016. URL `http://dx.doi.org/10.1051/eas/0936016`.

Massimo Meneghetti, Guido Davoli, Pietro Bergamini, Piero Rosati, Priyamvada Natarajan, Carlo Giocoli, Gabriel B. Caminha, R. Benton Metcalf, Elena Rasia, Stefano Borgani, Francesco Calura, Claudio Grillo, Amata Mercurio, and Eros Vanzella. An excess of small-scale gravitational lenses observed in galaxy clusters. 2020. URL `https://ludwig.lub.lu.se/login?url=https://search.ebscohost.com/login.aspx?direct=true&AuthType=ip,uid&db=edsarx&AN=edsarx.2009.04471&site=eds-live&scope=site`.

Mark H. Jones, Robert J.A. Lambourne, and Stephen Serjeant, editors. *An Introduction to Galaxies and Cosmology (Second Edition)*. Cambridge University Press, Cambridge, 2015.

Zhijie Xu. Cold dark matter particle mass and properties and axion-like dark radiation in λcdm cosmology, 2023.

T. K. Chan, D. Kereš, J. Oñorbe, P. F. Hopkins, A. L. Muratov, C.-A. Faucher-Giguère, and E. Quataert. The impact of baryonic physics on the structure of dark matter haloes: the view from the fire cosmological simulations. *Monthly Notices of the Royal Astronomical Society*, 454(3):2981–3001, October 2015. ISSN 1365-2966. doi: 10.1093/mnras/stv2165. URL http://dx.doi.org/10.1093/mnras/stv2165.

MPG. Putting the universe to the test. URL https://www.mpg.de/20761326/millennium-tng-cosmology-simulation.

Ji-hoon Kim, Tom Abel, Oscar Agertz, Greg L. Bryan, Daniel Ceverino, Charlotte Christensen, Charlie Conroy, Avishai Dekel, Nickolay Y. Gnedin, Nathan J. Goldbaum, Javiera Guedes, Oliver Hahn, Alexander Hobbs, Philip F. Hopkins, Cameron B. Hummels, Francesca Iannuzzi, Dusan Keres, Anatoly Klypin, Andrey V. Kravtsov, Mark R. Krumholz, Michael Kuhlen, Samuel N. Leitner, Piero Madau, Lucio Mayer, Christopher E. Moody, Kentaro Nagamine, Michael L. Norman, Jose Onorbe, Brian W. O'Shea, Annalisa Pillepich, Joel R. Primack, Thomas Quinn, Justin I. Read, Brant E. Robertson, Miguel Rocha, Douglas H. Rudd, Sijing Shen, Britton D. Smith, Alexander S. Szalay, Romain Teyssier, Robert Thompson, Keita Todoroki, Matthew J. Turk, James W. Wadsley, John H. Wise, Zolotov, and Adi. The agora high-resolution galaxy simulations comparison project. *The Astrophysical Journal Supplement Series*, 210(1):14, December 2014. ISSN 1538-4365. doi: 10.1088/0067-0049/210/1/14. URL http://dx.doi.org/10.1088/0067-0049/210/1/14.

AGORA. The agora project. URL https://sites.google.com/site/santacruzcomparisonproject/about?authuser=0.

Ji-hoon Kim, Oscar Agertz, Romain Teyssier, Michael J. Butler, Daniel Ceverino, Jun-Hwan Choi, Robert Feldmann, Ben W. Keller, Alessandro Lupi, Thomas Quinn, Yves Revaz, Spencer Wallace, Nickolay Y. Gnedin, Samuel N. Leitner, Sijing Shen, Britton D. Smith, Robert Thompson, Matthew J. Turk, Tom Abel, Kenza S. Arraki, Samantha M. Benincasa, Sukanya Chakrabarti, Colin DeGraf, Avishai Dekel, Nathan J. Goldbaum, Philip F. Hopkins, Cameron B. Hummels, Anatoly Klypin, Hui Li, Piero Madau, Nir Mandelker, Lucio Mayer, Kentaro Nagamine, Sarah Nickerson, Brian W. O'Shea, Joel R. Primack, Santi Roca-Fàbrega, Vadim Semenov, Ikkoh Shimizu, Christine M. Simpson, Keita Todoroki, James W. Wadsley, and John H. Wise. The agora high-resolution galaxy simulations comparison project. ii. isolated disk test. *The Astrophysical Journal*, 833 (2):202, December 2016. ISSN 1538-4357. doi: 10.3847/1538-4357/833/2/202. URL http://dx.doi.org/10.3847/1538-4357/833/2/202.

Santi Roca-Fàbrega, Ji-Hoon Kim, Loic Hausammann, Kentaro Nagamine, Alessandro Lupi, Johnny W. Powell, Ikkoh Shimizu, Daniel Ceverino, Joel R. Primack, Thomas R. Quinn, Yves Revaz, Héctor Velázquez, Tom Abel, Michael Buehlmann, Avishai Dekel, Bili Dong, Oliver Hahn, Cameron Hummels, Ki-Won Kim, Britton D. Smith, Clayton Strawn, Romain Teyssier, Matthew J. Turk, and AGORA Collaboration. The AGORA High-resolution Galaxy Simulations Comparison Project. III. Cosmological Zoom-in Simulation of a Milky Way-mass Halo. , 917(2):64, August 2021. doi: 10.3847/1538-4357/ac088a.

Santi Roca-Fàbrega, Ji hoon Kim, Joel R. Primack, Minyong Jung, Anna Genina, Loic Hausammann, Hyeonyong Kim, Alessandro Lupi, Kentaro Nagamine, Johnny W. Powell, Yves Revaz, Ikkoh Shimizu, Clayton Strawn, Héctor Velázquez, Tom Abel, Daniel Ceverino, Bili Dong, Thomas R. Quinn, Eun jin Shin, Alvaro Segovia-Otero, Oscar Agertz, Kirk S. S. Barrow, Corentin Cadiou, Avishai Dekel, Cameron Hummels, Boon Kiat Oh, Romain Teyssier, and The Agora Collaboration. The agora high-resolution galaxy simulations comparison project iv: Halo and galaxy mass assembly in a cosmological zoom-in simulation at $z \leqslant 2$, 2024.

Minyong Jung, Santi Roca-Fàbrega, Ji-hoon Kim, Anna Genina, Loic Hausammann, Hyeonyong Kim, Alessandro Lupi, Kentaro Nagamine, Johnny W. Powell, Yves Revaz, Ikkoh Shimizu, Héctor Velázquez, Daniel Ceverino, Joel R. Primack, Thomas R. Quinn, Clayton Strawn, Tom Abel, Avishai Dekel, Bili Dong, Boon Kiat Oh, and Romain Teyssier. The agora high-resolution galaxy simulations comparison project. v. satellite galaxy populations in a cosmological zoom-in simulation of a milky way–mass halo. *The Astrophysical Journal*, 964(2):123, March 2024. ISSN 1538-4357. doi: 10.3847/1538-4357/ad245b. URL `http://dx.doi.org/10.3847/1538-4357/ad245b`.

Clayton Strawn, Santi Roca-Fàbrega, Joel R. Primack, Ji-hoon Kim, Anna Genina, Loic Hausammann, Hyeonyong Kim, Alessandro Lupi, Kentaro Nagamine, Johnny W. Powell, Yves Revaz, Ikkoh Shimizu, Héctor Velázquez, Tom Abel, Daniel Ceverino, Bili Dong, Minyong Jung, Thomas R. Quinn, Eun-jin Shin, Kirk S. S. Barrow, Avishai Dekel, Boon Kiat Oh, Nir Mandelker, Romain Teyssier, Cameron Hummels, Soumily Maji, Antonio Man, and Paul Mayerhofer. The agora high-resolution galaxy simulations comparison project. vi. similarities and differences in the circumgalactic medium. *The Astrophysical Journal*, 962(1):29, February 2024. ISSN 1538-4357. doi: 10.3847/1538-4357/ad12cb. URL `http://dx.doi.org/10.3847/1538-4357/ad12cb`.

Douglas Scott. The standard model of cosmology: A skeptic's guide, 2018.

NASA/LAMBDAArchive/WMAPScienceTeam. cdm model of cosmology. URL `https://lambda.gsfc.nasa.gov/education/graphic_history/univ_evol.html`.

G. J. Ferland, R. L. Porter, P. A. M. van Hoof, R. J. R. Williams, N. P. Abel, M. L. Lykins, G. Shaw, W. J. Henney, and P. C. Stancil. The 2013 Release of Cloudy. , 49:137–163, April 2013. doi: 10.48550/arXiv.1302.4485.

Francesco Haardt and Piero Madau. Radiative Transfer in a Clumpy Universe. IV. New Synthesis Models of the Cosmic UV/X-Ray Background. , 746(2):125, February 2012. doi: 10.1088/0004-637X/746/2/125.

Gilles Chabrier. The Galactic Disk Mass Function: Reconciliation of the Hubble Space Telescope and Nearby Determinations. , 586(2):L133–L136, April 2003. doi: 10.1086/374879.

Andrey V. Kravtsov, Anatoly A. Klypin, and Alexei M. Khokhlov. Adaptive Refinement Tree: A New High-Resolution N-Body Code for Cosmological Simulations. , 111(1):73–94, July 1997. doi: 10.1086/313015.

Greg L. Bryan, Michael L. Norman, Brian W. O'Shea, Tom Abel, John H. Wise, Matthew J. Turk, Daniel R. Reynolds, David C. Collins, Peng Wang, Samuel W. Skillman, Britton Smith, Robert P. Harkness, James Bordner, Ji-hoon Kim, Michael Kuhlen, Hao Xu, Nathan Goldbaum, Cameron Hummels, Alexei G. Kritsuk, Elizabeth Tasker, Stephen Skory, Christine M. Simpson, Oliver Hahn, Jeffrey S. Oishi, Geoffrey C. So, Fen Zhao, Renyue Cen, Yuan Li, and Enzo Collaboration. ENZO: An Adaptive Mesh Refinement Code for Astrophysics. , 211(2):19, April 2014. doi: 10.1088/0067-0049/211/2/19.

Harshitha Menon, Lukasz Wesolowski, Gengbin Zheng, Pritish Jetley, Laxmikant Kale, Thomas Quinn, and Fabio Governato. Adaptive techniques for clustered n-body cosmological simulations, 2014.

Paul Bode and Jeremiah P. Ostriker. Tree particle-mesh: An adaptive, efficient, and parallel code for collisionless cosmological simulation. *The Astrophysical Journal Supplement Series*, 145(1):1–13, March 2003. ISSN 1538-4365. doi: 10.1086/345538. URL http://dx.doi.org/10.1086/345538.

Shohei Aoyama, Kuan-Chou Hou, Ikkoh Shimizu, Hiroyuki Hirashita, Keita Todoroki, Jun-Hwan Choi, and Kentaro Nagamine. Galaxy simulation with dust formation and destruction. , 466(1):105–121, April 2017. doi: 10.1093/mnras/stw3061.

Y. Revaz and P. Jablonka. The dynamical and chemical evolution of dwarf spheroidal galaxies with gear. *Astronomy amp; Astrophysics*, 538:A82, February 2012. ISSN 1432-0746. doi: 10.1051/0004-6361/201117402. URL http://dx.doi.org/10.1051/0004-6361/201117402.

Philip F. Hopkins. A general class of Lagrangian smoothed particle hydrodynamics methods and implications for fluid mixing problems. , 428(4):2840–2856, February 2013. doi: 10.1093/mnras/sts210.

Fabrice Durier and Claudio Dalla Vecchia. Implementation of feedback in smoothed particle hydrodynamics: towards concordance of methods: Towards concordance of feedback methods in sph. *Monthly Notices of the Royal Astronomical Society*, 419(1): 465–478, October 2011. ISSN 0035-8711. doi: 10.1111/j.1365-2966.2011.19712.x. URL http://dx.doi.org/10.1111/j.1365-2966.2011.19712.x.

Philip F. Hopkins. A new class of accurate, mesh-free hydrodynamic simulation methods. *Monthly Notices of the Royal Astronomical Society*, 450(1):53–110, 04 2015. ISSN 0035-8711. doi: 10.1093/mnras/stv195. URL https://doi.org/10.1093/mnras/stv195.

Volker Springel. E pur si muove:galilean-invariant cosmological hydrodynamical simulations on a moving mesh. *Monthly Notices of the Royal Astronomical Society*, 401(2):791–851, January 2010. ISSN 1365-2966. doi: 10.1111/j.1365-2966.2009.15715.x. URL http://dx.doi.org/10.1111/j.1365-2966.2009.15715.x.

Katy L. Proctor, Claudia del P. Lagos, Aaron D. Ludlow, and Aaron S. G. Robotham. Identifying the discs, bulges, and intra-halo light of simulated galaxies through structural decomposition, 2023.

Alis J. Deason and Vasily Belokurov. Galactic archaeology with gaia, 2024.

Matthew J. Turk, Britton D. Smith, Jeffrey S. Oishi, Stephen Skory, Samuel W. Skillman, Tom Abel, and Michael L. Norman. yt: A multi-code analysis toolkit for astrophysical simulation data. *The Astrophysical Journal Supplement Series*, 192(1):9, dec 2010. doi: 10.1088/0067-0049/192/1/9. URL `https://dx.doi.org/10.1088/0067-0049/192/1/9`.

Peter S. Behroozi, Risa H. Wechsler, and Hao-Yi Wu. The rockstar phase-space temporal halo finder and the velocity offsets of cluster cores. *The Astrophysical Journal*, 762(2): 109, December 2012. ISSN 1538-4357. doi: 10.1088/0004-637x/762/2/109. URL `http://dx.doi.org/10.1088/0004-637X/762/2/109`.

Jovan Veljanoski, Amina Helmi, Maarten Breddels, and Lorenzo Posti. Leaves on trees: identifying halo stars with extreme gradient boosted trees. *Astronomy amp; Astrophysics*, 621:A13, December 2018. ISSN 1432-0746. doi: 10.1051/0004-6361/201732303. URL `http://dx.doi.org/10.1051/0004-6361/201732303`.